Journal of New Technology and Materials (JNTM)
J. New Technol. Mater.
Vol. 10, N°02 (2020)10-17

OEB Univ. Publish. Co.

Synthesis, characterization of (Ag-SnO_2) nanoparticles and investigation of its antibacterial and anti-biofilm activities

Zahra Obeizi[a]*, Houneida Benbouzid[b], Tayeb Bouarroudj[c], Chahrazed Benzaid[d] and Abdelghani Djahoudi[e]

[a]*Laboratory of Biochemistry and Applied Microbiology, Department of Biochemistry ,Faculty of Sciences, University of Badji Mokhtar , Annaba 23000 , Algeria.*
[b]*Laboratory of Cellular Toxicology, Department of Biology, Faculty of Sciences, University of Badji Mokhtar , Annaba 23000, Algeria.*
[c]*Scientific and Technical Research Center in Physico-Chemical Analysis (CRAPC), Tipaza42004, Algeria.*
[c]*Environmental Research Center (CRE), Annaba23001, Algeria.*
[d] *Department of Biochemistry, Faculty of Sciences, University of Badji Mokhtar , Annaba 23000 , Algeria.*
[e]*Laboratory of Microbiology, Department of Pharmacy, Faculty of Medicine, University of Badji Mokhtar, Annaba 23000, Algeria.*

*Corresponding author, email: zahra24abeizi@gmail.com

Received date: May 30, 2020 ; revised date: Sep. 29, 2020 ; accepted date: Nov. 09, 2020

Abstract

Silver-doped tin oxide (Ag-doped SnO_2) nanoparticles (NPs) were manufactured by using chemical co-precipitation method. The synthesized Ag-doped SnO_2 nanoparticles were characterized by using X-Ray Diffraction (XRD) analysis, Dynamic Light Scattering (DLS), Fourier-transform infrared spectroscopy (FTIR), Scanning Electron Microscopy (SEM), Energy-dispersive X-ray spectroscopy (EDX) and Ultraviolet-visible (UV-Vis) spectroscopy. The antibacterial activity of the prepared Ag-SnO_2 nanoparticles was carried out by agar well diffusion method and determination of minimum inhibitory concentration against both Gram-negative (Escherichia coli, Pseudomonas aeruginosa, Klebsiella pneumoniae) and Gram-positive bacteria (Staphylococcus aureus, Bacillus cereus, Enterococcus faecalis), anti-biofilm activity was investigated using 96-well microtiter plate method against Staphylococcus aureus and Pseudomonas aeruginosa. XRD Results confirm formation of Ag-doped SnO_2 nanoparticles, the average grain size was found to be 23 nm; while DLS analysis indicates an average size around 29 nm. Morphological findings by SEM indicate dense particles with sponge-like microstructure that are uniformly organized irregularly, The EDX analysis confirms the purity of these nanoparticles with peaks of Ag, Sn, and O atoms. SnO_2-Ag NPs were exhibited good antibacterial activity against all bacterial strains tested with maximum zone of inhibition of 27 ± 1.2 mm for S. aureus, the minimum inhibitory concentration values varied between 8 and 128 µg / ml. The significant percentage of biofilm inhibition was found 73.96% and 71.19% against S. aureus and P. aeruginosa biofilm, respectively.

Keywords: Co-precipitation method; Ag-SnO_2 nanoparticles; Antibacterial; Anti-biofilm; Minimum inhibitory concentration.

1. Introduction

Nanotechnology is widely used in several medical fields especially diagnosis of diseases and preparation of drugs.[1;2] Nanoparticles of metal oxides such as zinc oxide (ZnO), manganese oxide (MgO), titanium oxide (TiO_2), and iron oxide (Fe_2O_3) are widely relevant in biological applications because of its particular physiochemical characteristics [3].

Tin oxide (SnO_2) is an n-type semiconductor with a broad Eg = 3.6eV band gap used for prospective catalytic applications, gas sensors, dye-based solar cells and clear conductive electrode. [4] In addition to these notable applications, this metal oxide was also researched for antimicrobial study, *E. coli* (Gram-negative) and *S. aureus* (Gram-positive) have been recorded to be inactivated in MilliQ water by SnO_2 nanoparticles. [5;6] Before large use of antibiotics, several metals, such as silver (Ag), zinc (Zn), copper (Cu) and magnesium (Mg) have historically been used to kill bacteria. [7;8] Ag used as doping agent for nanoparticles enhanced their antibacterial activity and changed their mechanical properties. [9] Previous studies have demonstrated that silver doped nanomaterials have excellent bactericidal effect. [10;11] A recent study carried out by Wu et al (2019) showed that there are synergistic effects of Ag + and reactive oxygen species (ROS) can accelerate the death of bacteria by destroying biomolecules. [12] Herein, it should be highlighted that, despite many studies were mentioned in the literature about antibacterial activity of Co-SnO_2, [13;14] they are rare or very limited on AgdopedSnO_2.

Nosocomial infections are triggered a great deal of morbidity, death and enhanced economic stress. One of the factors for these alarming diseases is the present misuse of antimicrobial agents in clinics that create durable multi-resistant bacteria species [15]. Antibiotic resistance is

growing rapidly and is a major concern. Therefore, antibiotic resistance must be reduced which requires to renew research efforts to search for alternatives to antibiotics, nanomaterials (particularly nanogold and nanosilver) are becoming effective and efficient antibacterial agent for curing human diseases [16;17].

Biofilms are liable for many chronic diseases and it has become very hard to control them efficiently due to the advent of antibiotic-resistant bacteria. The bacteria's biofilm matrix allows them tolerant severe conditions and antibacterial therapies [18]. Therefore, it is crucial to develop novel anti-biofilm molecules that can efficiently minimize and eradicate diseases associated with biofilms.

In this research, SnO_2 has been doped particularly with Ag in order to maximize its antibacterial activity. Ag-doped SnO_2 NPs have been prepared by chemical co-precipitation method, followed by characterization using XRD, DLS, FT-IR, SEM, EDX and UV-Vis. Antibacterial and anti-biofilm activities have been performed on a large number of multidrug-resistant bacterial strains isolated from various pathological samples of patients and hospital environment.

2. Experimental

2.1. Chemicals and bacterial strains

The chemicals used were obtained from Sigma-Aldrich. Bacterial strains were provided by the General Microbiology Laboratory, Faculty of Medicine, Badji Mokhtar University of Annaba, directed by Professor DJAHOUDI A.E.G.

2.2. Preparation of Ag-SnO_2 nanoparticles

The technique of co-precipitation was used to prepare Ag-SnO_2 nanoparticles. An appropriate amount of $AgNO_3$ is added to 8 g of stannous chloride ($SnCl_4.5H_2O$) to reach 5%, dissolved in a minimum amount of double distilled water, and then aqueous NH_3 is added to the mixture until the solution pH reaches 7. The Formed precipitate was stirred at room temperature for 3 hours and then washed several times with double-distilled water to remove NO_3 and Cl ions. Finally, the as-obtained product is dried at 300°C for 2 hours in a hot air oven followed by calcination at 800°C for 3 hours in order to achieve fine powder.

2.3. Characterization of Ag-doped SnO_2 Nanoparticles

Characterization of prepared Ag-SnO_2 nanoparticles was performed by X-ray diffraction using Panalytical X'PERT diffractometer with CuKα radiation source (π = 1,5418 Å) and 40 kV/30 mA voltage / current operation to determine crystalline structure and average grain size of Ag-SnO_2 NPs. Dynamic light scattering (DLS) was used to measure the size of NPs using MALVERN type NANO-ZS. Fourier Transform Infra-Red Spectroscopy (FT-IR) was employed to determine the functional group using SHIMADZU FTIR-8400S. Scanning Electron Microscopy (ZEISS SEM) noted the morphologies of prepared composites. Using Jenway 6405 Uv/vis spectrophotometer, in the spectrum 200 – 800 nm, the optical characteristics of nanoparticles were examined. Energy Dispersive X spectrum (EDAX) is registered using EDAX AMETEK Smart Insight to check NPs purity.

2.4. Agar well diffusion method

The antibacterial activity of Ag-doped SnO_2 nanoparticles on the growth of *Gram-negative (Escherichia coli, Pseudomonas aeruginosa, Klebsiella pneumoniae) and Gram-positive (Staphylococcus aureus, Bacillus cereus, Enterococcus faecalis)* pathogenic bacteria was checked by agar well diffusion method. Gentamicin (10µg/ml) was taken as positive control and Dimethyl sulfoxide (DMSO) served as negative control. Solution of SnO_2-Ag nanoparticles at concentration of 1 M was prepared in DMSO by ultra-sonication. The turbidity of bacterial inoculums was adjusted to 0.5 McFarland (10^8 colony forming units (CFU)/ml) corresponding to an optic density of 0.08 to 0.1 read at 625nm after mixing a few colonies of 24 hours old culture of each bacterial strain with sterile physiological saline. Bacterial inoculums were spread using sterilized cotton swab on Petri dishes prepared with Muller Hinton Agar and containing three wells of 6 mm of diameter. After, the wells were loaded with Gentamicin, solution of NPs and DMSO respectively. The plates were incubated at 37°C for 24 h. All assays have been conducted in triplicates. The antibacterial activity was evaluated by measuring the diameter of the zone of inhibition formed around the well.

2.5. Determination of minimum inhibitory concentration

The Minimum inhibitory concentration (MIC) represents the lowest concentration totally inhibiting bacterial growth visible after 24 h of incubation at 37°C [19]. MIC of Ag-SnO_2 NPs was determined by the micro dilution method. Gram positive and Gram negative bacteria were cultured on Nutrient agar at 37°C for 18 h. Inoculum of organisms should be prepared to10^5CFU/ml. A stock solution of NPs at a concentration of 1024 µg/ml was prepared, followed by sonication and autoclaving at 121°C during 30 minutes. Semi-log dilutions of half-to-half in sterile distilled water were prepared (512, 256,128, 64, 32, 16, 8, 4, 2, 1 and 0.5) µg/ml. 2 ml of each concentration was mixed with18 ml of Muller Hinton agar to prepare petri dishes. After solidification of the medium, 2 µl of each inoculum was deposited on the broth media. After that, the petri dishes were left at room temperature until the moisture was absorbed (spot drying, no more

than 30 minutes), and then the dishes were incubated at 37°C for 18-24 hours.

2.6. *96-well microtiter plate method*

Anti-biofilm activity of Ag-doped SnO_2 NPs was determined against *Staphylococcus aureus* and *Pseudomonas aeruginosa*, using 96-well microtiter plate method according to [20]. All biofilm experiments were repeated three times. The turbidity of overnight grown bacterial cultures in the medium Brain Heart Infusion Brown (BHIB) was adjusted to 0.5 McFarland. In the wells of microplate, 100 µl of each bacterial suspension was mixed with equal volume of solution of synthesized Ag-SnO_2 nanoparticles having different concentrations (8, 16, 32 and 64 µg/ mL), incubation is performed at 37°C for 24 h. The control test includes wells containing inoculum without NPs and the wells containing only the growth medium as positive control and negative control respectively. After incubation, the culture supernatant was discarded, and wells of microplate were washed three times with buffer saline phosphate (PBS) to remove non-adherent cells and the adherent bacteria on the plate were subjected to 200 µl of 0.1% violet crystal solution (w / v) for 30 min. Then microplate was washed three times with demineralized water to remove the excess crystal violet and dried at room temperature. After that, 200 µl of ethanol-acetone mixture (75/25%) was added to each well for 30 min. Biofilm inhibition was determined by recording optical density (OD) at 595 nm using microplate reader (FilterMax F5 ELIZA) and calculate biofilm inhibition rate using the equation given below:

$$Biofilm\ inhibition\ (\%) = (OD\ Positive\ Control - OD\ Concentration\ Test\ )/(OD\ Positive\ Control) \times 100$$

3. Results

3.1. *X-ray Diffraction Studies and DLS analysis*

The X-ray diffraction patterns shown in Figure 1 reveal well-defined peaks with relatively lower intensity, an indication of the formation of nanocrystalline phase. Phase identification reveals the formation of pure tetragonal rutile-type structure of SnO_2 phase with space group P42/mnm, in good agreement with the literature [21]. The observed reflections are indexed (110), (101), (200), (111), (210), (211), (220), (002), (310), (112), (301), (202), (321) and (400) in accordance with JCPDS card No. 41-1445. No additional peaks belonging to Ag or its oxides can be detected. The average crystallite sizes of the pure and Ag doped SnO_2 nanoparticles were calculated by the Scherrer equation: $D=k\lambda/\beta\cos\theta$, where D is the crystallite size, K=0.9, λ is the X-ray wavelength, β is the full width at half maximum of the diffraction peak, and θ is the Bragg diffraction angle of the diffraction peaks. The peak used to determine the crystallite size is the intense peak (110).The calculated crystallite size was found to be 13 nm for SnO_2 then increases significantly with Ag-doping by more than twice reaching 23 nm. This indicates that Ag favors grain refinement during synthesis process.

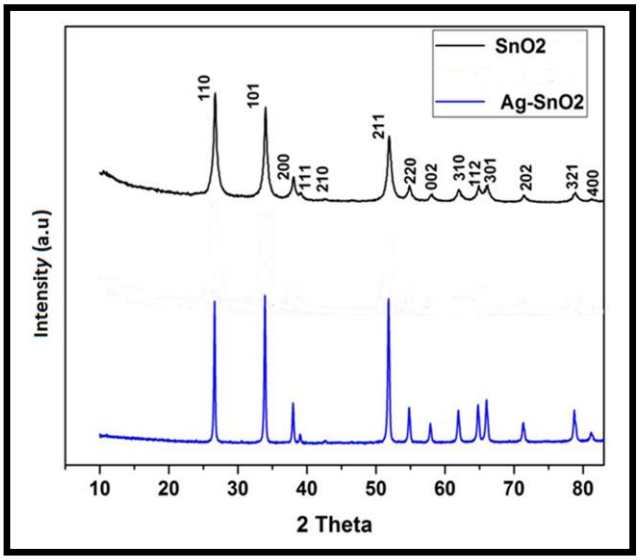

Figure 1. X-ray diffraction patterns of pure and Ag doped SnO_2 NPs

Dynamic light scattering (DLS) determined particle size. The average size of Ag-SnO_2 NPs was determined 29.28 nm. (Figure2)

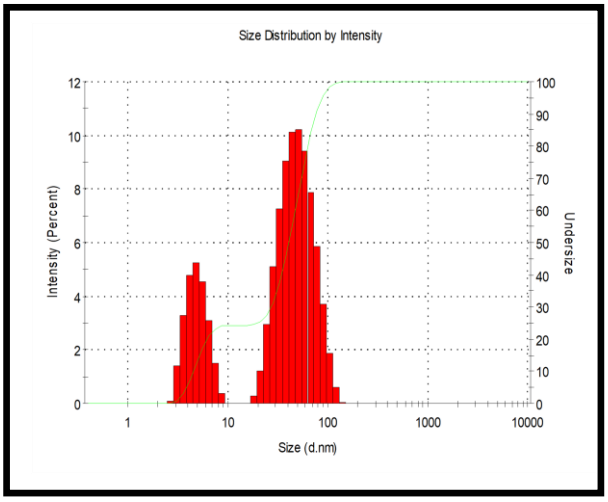

Figure 2. Size measurement of the prepared Ag-SnO_2 NPs.

3.2. Scanning Electron Microscopy and EDX analysis

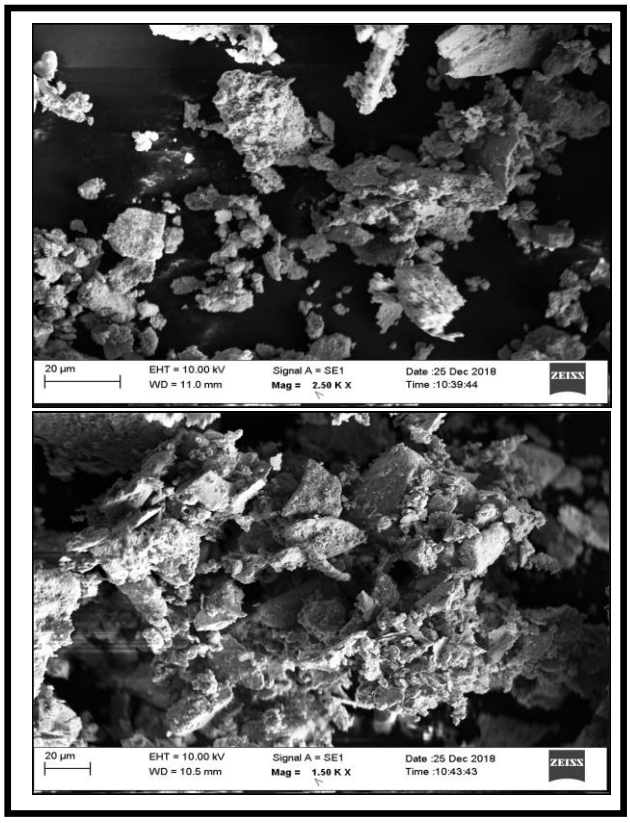

Figure 3. SEM Images of Ag doped SnO_2 NPs.

Figure3 displays SEM micrographs of the synthesized Ag-SnO_2 nanoparticles. It reveals randomly arranged irregular sized compact grains with sponge like structure. Some spongy grains are overgrown on the compact sticky grains, with the presence of some deep pits. Clustering (agglomeration) of very fine particles occurred on the surface of large particles.

The energy dispersive X-ray spectrum (Figure 4) reveals three elements Ag, Sn and O, which indicate the purity of Ag-SnO_2 nanoparticles.

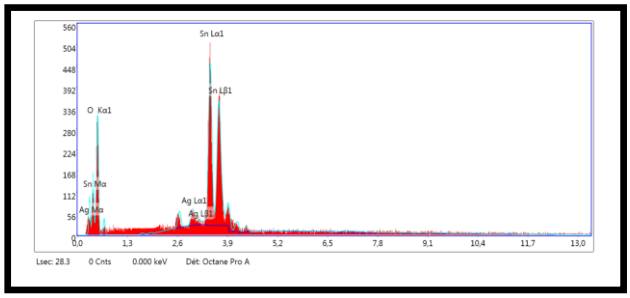

Figure 4. EDX spectrum of Ag doped SnO_2 NPs

3.3. Fourier Transform Infrared Spectroscopy

The FTIR spectroscopy analysis of chemically synthesized nanocomposites revealed that the two spectra are quite similar, as shown in Figure 5. Three IR absorption zones can be identified in the FT-IR spectra: (i) the absorption band located in the range 1628 - 3421 cm^{-1} can be attributed to the vibrations of the binding of the absorbed molecular water and the vibrations of the hydroxyl groups [22]; (ii) the second band appearing in the range of 400 - 700 cm^{-1}, particularly at 633 cm^{-1} is ascribed to Sn-O-Sn and Sn-O antisymmetric vibrations stretching on the surface of the oxide bridge formed by vibrational condensation of the adjacent surface of hydroxyl group [23]; and finally (iii) the absorption band in the range 3300 - 3475 cm^{-1} (3442 cm^{-1}) can be associated to the vibration of the OH hydroxyl group bond of the absorbed molecular water on the surface of SnO_2 [24].

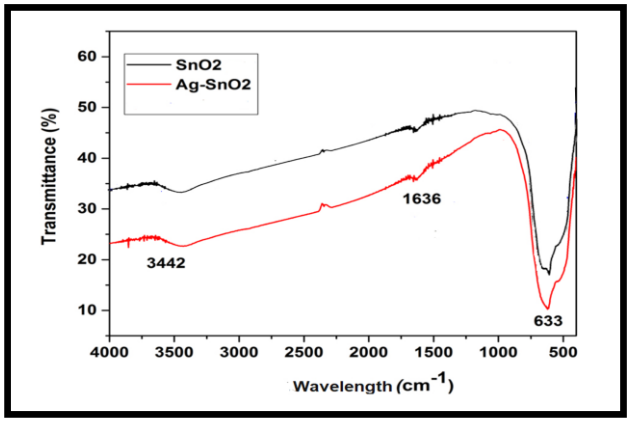

Figure 5. FT-Infrared spectra of pure and Ag-SnO_2 NPs.

3.4. Ultraviolet-visible spectroscopy

The UV-vis spectra as shown in Figure 6 clearly reveal that the wavelengths associated with the maximum absorbance values vary, as well as the pseudo-trays of minimal absorbance. In addition, it is observed that the absorption is shifted toward higher wavelength values for Ag doped compared to pure SnO_2; known as red-shift and hence confirming the dissolution of Ag^+ within SnO_2 host lattice by occupying Sn^{4+} sites.

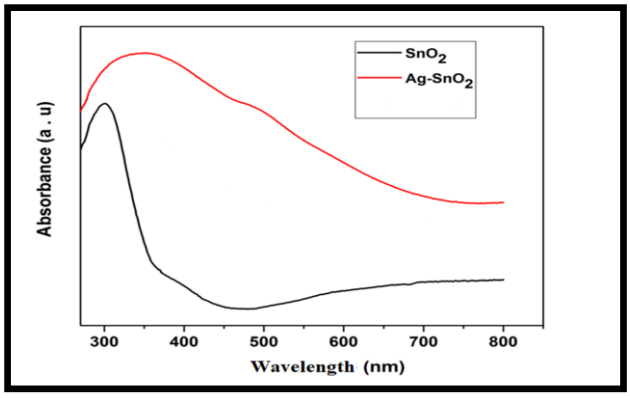

Figure 6. Optical Absorbance of Pure and Ag doped SnO_2 NPs.

3.5. Antibacterial activity

The antibacterial activity of Ag doped SnO_2 NPs against Gram negative and Gram positive multi resistant bacteria have been estimated (Figure 7). Results exhibited considerable growth inhibition of all bacterial strains by Ag-SnO_2 nanoparticles compared to control. The presence of Ag-SnO_2 NPs in the bacterial medium induce the secretion of reactive oxygen species (ROS) which allows NPs to penetrate the cell membrane and inactivate bacteria; this bactericidal power develops with the increase of the concentration of NPs. [25] Assuming that the interactions between Ag + ions and negatively charged groups present on the bacterial walls cause major structural damage, including holes. This increases the membrane permeability and facilitates the exit of cellular constituents as well as the penetration of Ag + ions into the cell. The flow of these Ag + ions form bonds with the biological molecules containing the thiol group (-SH); cause an alteration of the intracellular enzymatic activity and a release of K + ions (elements necessary to maintain the internal osmotic pressure) [26] and interact with the enzymes of the respiratory chain (example: NADH dehydrogenase) and prevent the transport of electrons from one complex to another in this chain [27]. All of these phenomena lead to the death of the bacteria. Our results are similar to those of Qamar et al (2017) [28] who found that the nanoparticles of Co- SnO_2 exhibit significant antibacterial activity against *B. subtilis* and *E. coli* with zone of inhibition of (16 and 22) mm respectively.

Table1: Mean zone of inhibition of bacterial strains by Ag-SnO_2 NPs

Bacterial strains	Zone of Inhibition (mm)		
	Ag-SnO_2NPs (1M)	Gentamicin positive control	DMSO negative control
S. aureus	27 ± 1.2	20 ± 1.1	-
E. coli	25 ± 0.8	15 ± 0.3	-
K. pneumoniae	26 ± 0.6	13 ± 0.9	-
P. aeruginosa	22 ± 0.9	14 ± 0.2	-
E. faecalis	27 ± 0.4	19 ± 1.4	-
B. cereus	23 ± 0.7	12 ± 0.5	-

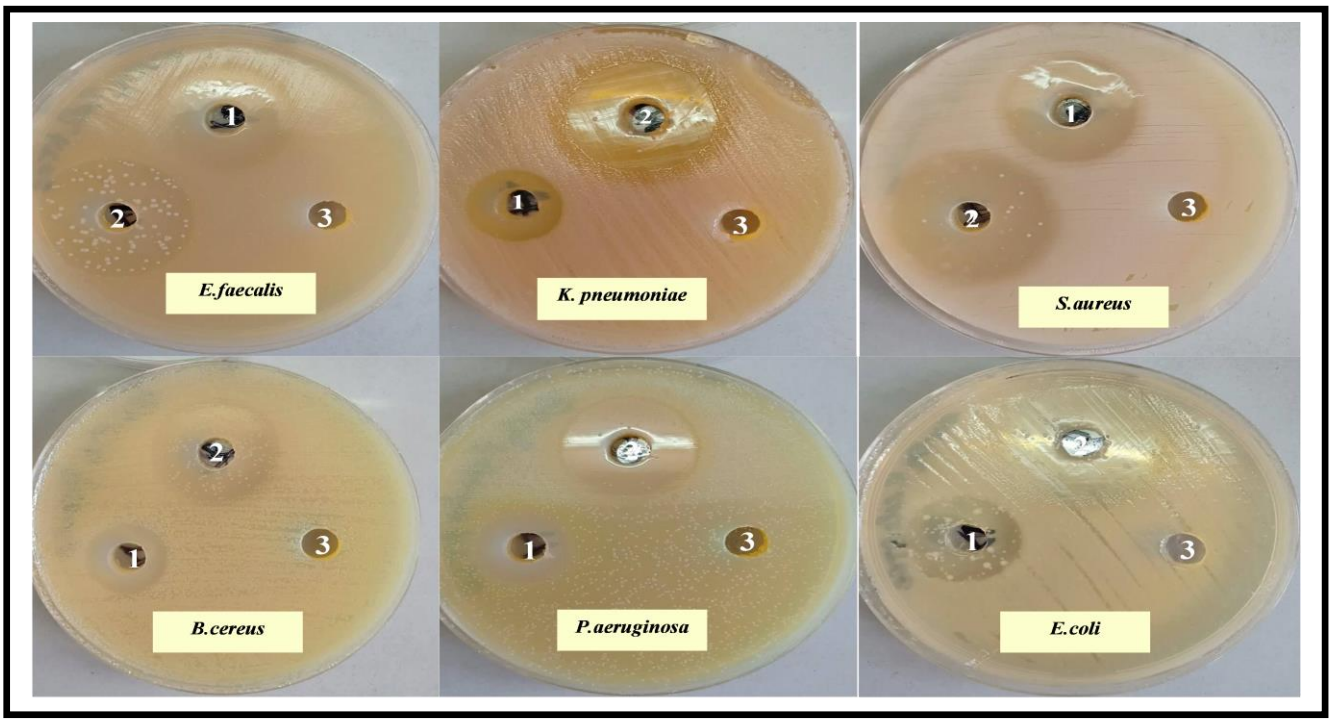

Figure 7. Antibacterial activity of Ag doped SnO_2 NPs.1: Gentamicin, 2: Solution of Ag-SnO_2 NPs, 3: DMSO

Antibacterial activity of these Ag-SnO_2 synthesized NPs was also evaluated using standard dilution method, which consists on the determination of the minimum concentration of the tested molecule necessary to inhibit the growth of the bacteria tested. The final MIC values are listed in Figure 8. The MIC values fall within the range from 8 µg/ml to 128 µg/ml. A lower MIC demonstrates great antibacterial effectiveness.

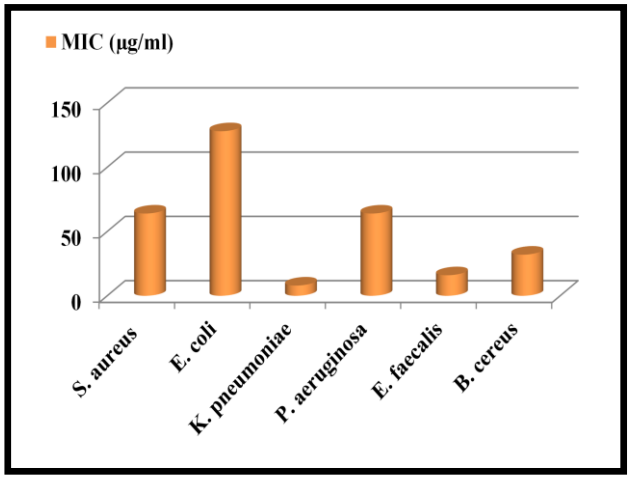

Figure 8. MIC values of bacterial strains treated with Ag doped SnO_2 NPs.

3.6. Anti-biofilm activity

Ag-SnO_2 NPs have been able to reduce biofilm formation of strains tested as shown in Figure 9. The obtained inhibition rate with *Staphylococcus aureus* strain is about 73.96%, whereas for the strain *Pseudomonas aeruginosa* is in the order of 71.19%. Al-Shabib et *al* (2018) [29] demonstrated that Tin Oxide hollow nanoflowers exhibited significant inhibition of quorum sensing regulated virulence and biofilm formation of pathogenic bacteria (*Serratia marcescens*, *Chromobacterium violaceum* and *Pseudomonas aeruginosa*). Gurunathan et al (2014) [30] observed the inhibition of the growth of biofilms formed by human pathogens: *S. pneumoniae*, *S. flexneri*, *P. aeruginosa* and *S. aureus* treated with Ag NPs at concentrations ranging from 0.1 to 1 µg / ml. Our results are encouraging and confirm the effective eradication of biofilms formed by *S. aureus* and *P. aeruginosa* by Ag-SnO_2NPs.

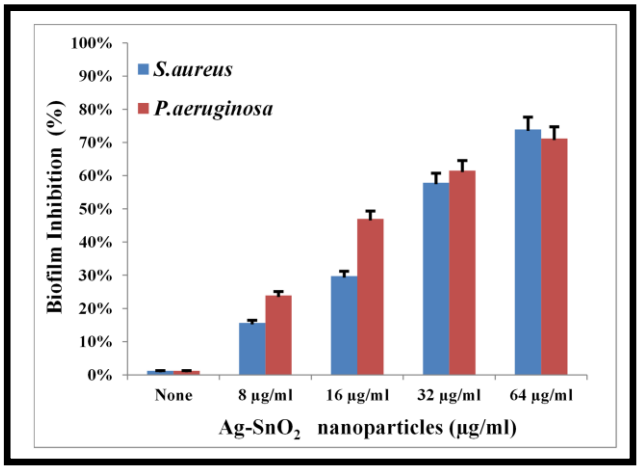

Figure 9. Anti-Biofilm activity of Ag doped SnO_2 NPs.

Acknowledgments

The authors thank Department of Genetics and Bioengineering, Yeditepe University Istanbul, Turkey for performing SEM and DLS characterization studies.

4. Conclusion

The results of this research work indicate that doping influenced physical characteristics of synthesized nanoparticles by modification of surface (large surface area with increase grain size but smaller particle size), which enhanced the antibacterial and anti-biofilm properties. In conclusion, Ag-SnO_2 NPs are found to be potentially exploiting as efficient alternative to combat antibiotic resistance in pharmaceutical field.

References

[1] N. L. Gavade, A. N. Kadam, M.B. Suwarnkar, V.P. Ghodake, K.M. Garadkar, Biogenic synthesis of multi-applicative silver nanoparticles by using Ziziphus Jujuba leaf extract, Spectrochim Acta A Mol Biomol Spectrosc.136 (2015) 953–960

[2] J. K. Patra, K.H. Baek, Green biosynthesis of magnetic iron oxide (Fe3O4) nanoparticles using the aqueous extracts of food processing wastes under photo-catalyzed condition and investigation of their antimicrobial and antioxidant activity. J Photoch Photobio B. 173 (2017) 291–300

[3] M. Sundrarajan, K. Bama, M. Bhavani, S. Jegatheeswaran, S. Ambika, A. Sangili, P. Nithya, R. Sumathi, Obtaining titanium dioxide nanoparticles with spherical shape and antimicrobial properties

using M. citrifolia leaves extract by hydrothermal method. J Photoch Photobio B.171(2017)117–124

[4] A. Bhattacharjee, M. Ahmaruzzaman, T. Sinha, A novel approach for the synthesis of SnO2 nanoparticles and its application as a catalyst in the reduction and photodegradation of organic compounds, , Spectroc. Acta A.136 (2015) 751–760

[5] M. M. Rashad, A. Ismail, I. Osama, I.A. Ibrahim, A-H.T. Kandil, Photocatalytic decomposition of dyes using ZnO doped SnO2 nanoparticles prepared by solvothermal method, Arab. J. Chem. 7(1) (2014) 71–77

[6] S. M. Amininezhad, A. Rezvani, M. Amouheidari, S. M. Amininejad , S. Rakhshani, The antibacterial activity of SnO2 nanoparticles against Escherichia coli and Staphylococcus aureus, Zahedan J.Res.Med.Sci. 17(9) (2015)1-5

[7] J. A. Lemire, J. J. Harrison, R. J Turner, Antimicrobial activity of metals: mechanisms, molecular targets and applications. Nat. Rev. Microbiol. 11(6) (2013) 371-384.

[8] A. Sirelkhatim, S. Mahmud, A. Seeni, N. Kaus, L. C, Ann, S. Bakhori, H. Hasan, D. Mohamad Review on Zinc Oxide Nanoparticles: Antibacterial Activity and Toxicity Mechanism. Nano-Micro Lett. 7(3) (2015).219-242.

[9] H. B. Dias, M.I. B, Bernardi, V.S. Marangoni, A.C. de Abreu Bernardi, A. N, de Souza Rastelli, A. C. Hernandes, Synthesis, characterization and application of Ag doped ZnO nanoparticles in a composite resin. Mater Sci Eng C Mater Biol Appl, 96(2018) 391-401.

[10] R. D. Holtz, B.A. Lima, A.G. Souza Filho, M. Brocchi, O.L. Alves, Nanostructured silver vanadate as a promising antibacterial additive to water-based paints. Nanomedicine, 8(6) (2012) 935–940.

[11] Y. Li, S. Gao, B. Zhang, H. Mao, X. Tang, Electrospun Ag-Doped SnO2 Hollow Nanofibers with High Antibacterial Activity. Electron. Mater. Lett. 16 (2020)195–206.

[12] Y. Wu, L. Zhang, Y. Zhou, L. Zhang, Y. Li, Q. Liu, J. Yang, Light-induced ZnO/Ag/rGO bactericidal photocatalyst with synergistic effect of sustained release of silver ions and enhanced reactive oxygen species. Chinese J. Catal, 40(5)(2019) 691–702.

[13] S. A. Khan, S. Kanwal, K. Rizwan, S. Shahid, Enhanced antimicrobial, antioxidant, in vivo antitumor and in vitro anticancer effects against breast caner cell line by green synthesized un-doped SnO2 and Co-doped SnO2 nanoparticles from Clerodendrum inerme, Microb. Pathog. 125 (2018) 366-384..

[14] D. Chandran, L.S. Nair, S. Balachandran, K. Ajendra Babu, M. Deepa, Structural, optical, photocatalytic, and antimicrobial activities of cobalt-doped tin oxide nanoparticles. J Sol-Gel Sci Technol 76(2015) 582–591.

[15] A. Revelas, Healthcare - associated infections: A public health problem. Niger Med J 53(2) (2012) 59-64

[16] A. MacGowan, E. Macnaughton, E; 2017. Antibiotic resistance. Med. 45(10) (2017) 622–628

[17] L. F. Alain, Antibiotics and Antibiotic Resistance. B.J.S.T.R. 1 (1) (2017) 65-80

[18] R. Roy, M. Tiwari, G. Donelli, V. Tiwari, Strategies for combating bacterial biofilms: A focus on anti-biofilm agents and their mechanisms of action. Virulence, 9(1)(2017) 522–554

[19] M. Curcic, M. Stankovic, I. Radojevic, O. Stefanovic, L.J. Comic, M. Topuzovic, D.S. Djacic, S.D. Markovic, Biological effects, total phenolic content and flavonoid concentrations of fragrant yellow onion (Allium flavum L.), Med. Chem. 8 (1) (2012) 46–51

[20] J. Saising, L. Dube, A.K. Ziebandt, S.P. Voravuthikunchai, M. Nega, F. Götz, Activity of Gallidermin on Staphylococcus aureus and Staphylococcus epidermidis Biofilms. Antimicrob Agents Ch, 56(11) (2012) 5804–5810

[21] E. P, Ganesh, d .K Dnyaneshwar, B.G.Vishwas and H.J Gotan. Preparation and characterization of SnO2 nanoparticles by hydrothermal route. Int. Nano Lett. 2 (1) (2012)17- 21

[22] L. K Bagal, J.Y PatilI, S. Mulla and S.S Suryavanshi. Influence of Pd-loading on gas sensing characteristics of SnO2 thick films. Ceram. Int., 38(6) (2012) 4835–4844.

[23] M. P Deosarkar, S.M Pawar, S.H Sonawane and B.A Bhanvase. Process intensification of uniform loading of SnO2 nanoparticles on graphene oxide nanosheets using a novel ultra sound assisted in situ chemical precipitation method. Chem Eng Process, 70 (2013) 48–54.

[24] J. Mazloom and F.E Ghodsi. Spectroscopic, microscopic, and electrical characterization of nanostructured SnO2: Co thin films prepared by sol–gel spin coating technique. Mater. Res. Bull , 48(4) (2013) 1468–1476.

[25] V. K Vidhu and D. Philip. Biogenic synthesis of SnO2 nanoparticles: Evaluation of antibacterial and antioxidant activities. , Spectroc. Acta A, 134 (2015) 372–379

[26] W. K Jung, H. C Koo, K. W Kim, S Shin, S. H Kim and Y. H Park. Antibacterial Activity and Mechanism of Action of the Silver Ion in Staphylococcus aureus and Escherichia coli. Applied and Environmental Microbiology, 74(7)(2008) 2171–2178.

[27] K. B Holt and A. J Bard. Interaction of Silver (I) Ions with the Respiratory Chain of Escherichia coli: An Electrochemical and Scanning Electrochemical Microscopy Study of the Antimicrobial Mechanism of Micromolar Ag+. Biochemistry, 44(39) (2005)13214–13223.

[28] M. A. Qamar, S. Shahid, S. A. Khan, S. Zaman, M. N. Sarwar. Synthesis characterization, optical and antibacterial studies of Co-Doped SnO2 nanoparticles. Dig. J Nanomater Bios, 12(4) (2017) 1127-1135

[29] N. A Al-Shabib, F.M Husain, N. Ahmad, F.A Qais, A. Khan, A. Khan, M.S. Khan, J. M. Khan, S.A. Shahzad, I. Ahmad. Facile Synthesis of Tin Oxide Hollow Nanoflowers Interfering with Quorum Sensing-Regulated Functions and Bacterial Biofilms. J. Nanomater, (2018) 1–11.

[30] S. Gurunathan, J. Han, D.N Kwon and J.H Kim,. Enhanced antibacterial and anti-biofilm activities of silver nanoparticles against Gram-negative and Gram-positive bacteria. Nanoscale Research Letters, 9(1) (2014) 373-389.